

## Parameter identification for nonlinear behavior of RC bridge piers using sequential modified extended Kalman filter

Kyoung Jae Lee<sup>\*1,2</sup> and Chung Bang Yun<sup>2</sup>

<sup>1</sup>Civil Engineering Team, Daelim Industrial Co. Ltd., 17-5 Yoido-dong, Youngdungpo-gu, Seoul 150-010, Korea

<sup>2</sup>Department of Civil and Environmental Engineering, Korea Advanced Institute of Science and Technology, 373-1 Gusong-dong, Yuseong-gu, Daejeon 305-701, Korea

(Received May 9, 2007, Accepted July 20, 2007)

**Abstract.** Identification of the nonlinear hysteretic behavior of a reinforced concrete (RC) bridge pier subjected to earthquake loads is carried out based on acceleration measurements of the earthquake motion and bridge responses. The modified Takeda model is used to describe the hysteretic behavior of the RC pier with a small number of parameters, in which the nonlinear behavior is described in logical forms rather than analytical expressions. Hence, the modified extended Kalman filter is employed to construct the state transition matrix using a finite difference scheme. The sequential modified extended Kalman filter algorithm is proposed to identify the unknown parameters and the state vector separately in two steps, so that the size of the problem for each identification procedure may be reduced and possible numerical problems may be avoided. Mode superposition with a modal sorting technique is also proposed to reduce the size of the identification problem for the nonlinear dynamic system with multi-degrees of freedom. Example analysis is carried out for a continuous bridge with a RC pier subjected to earthquake loads in the longitudinal and transverse directions.

**Keywords:** sequential modified extended Kalman filter; nonlinear system identification; hysteretic behavior of RC pier; the modified Takeda model; modal sorting; acceleration measurement only.

---

### 1. Introduction

For the health monitoring of civil infrastructures, it is important to identify the nonlinear behavior related to structural damage. Various system identification techniques are available for the identification of nonlinear structural dynamic systems. For the identification of structural parameters and their variations related to the nonlinear behavior, time domain analyses have been used widely, in particular methods of the least-square estimation (LSE) (Lee and Yun 1991, Loh and Lee 1997, Smyth, *et al.* 1999, Yang and Lin 2005) and the filtering approaches including the extended Kalman filter (EKF) (Yun and Shinozuka 1980, Hoshiya and Saito 1984, Loh and Chung 1993, Sato and Takei 1998, Yang, *et al.* 2006),  $H_\infty$  filter (Sato and Qi 1998), and Monte Carlo filter (Yoshida and Sato 2002, Sato and Chung 2005).

The forces induced on a bridge structure with reinforced concrete (RC) piers during major earthquakes may exceed the yield capacity of some piers and cause large inelastic deformations and

---

\*General Manager and Graduate Student, E-mail: lkjooo@daelim.co.kr

‡Professor, ycb@kaist.ac.kr

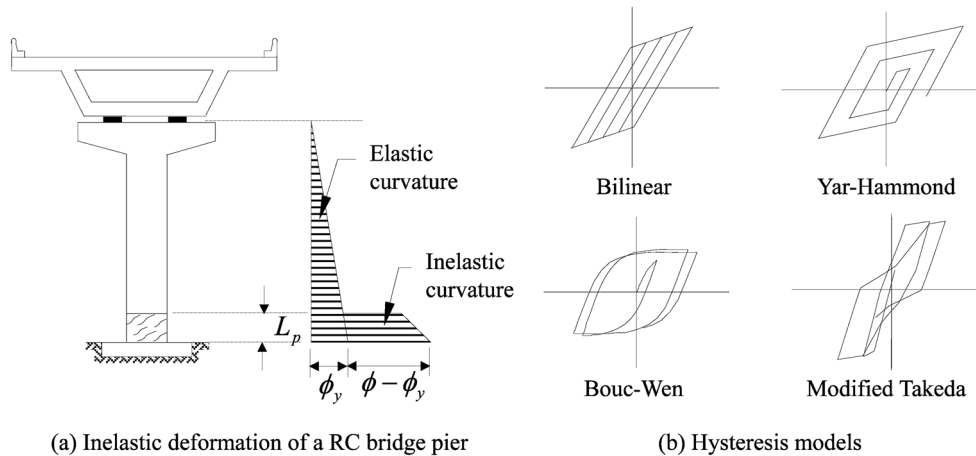


Fig. 1 Hysteretic behavior of a RC bridge pier

damages in the piers as depicted in Fig. 1(a). Since the seismic response of the bridge structure is highly affected by the hysteretic behavior of the damaged RC pier, reliable models for such behavior are needed. However some models that were derived from the detail information of the material and sectional characteristics are prohibitively expensive, and in many cases such refined nonlinear models may not be necessary in a global response evaluation (Umemura and Takizawa 1982). Various mechanical models have been proposed for the hysteretic behavior of RC structures (Clough, *et al.* 1965, D'Ambrisi and Fillippou 1999, Kwak, *et al.* 2004). Such models shall include important characteristics of damaged RC members such as stiffness degradation, pinching effect, and strength deterioration (Takeda, *et al.* 1970, Meyer, *et al.* 1983). The modified Takeda model (Roufaiel and Meyer 1987) can effectively reproduce such complex nonlinear hysteretic behavior of RC members with a limited number of parameters. So it has been widely used for concrete structures. Differently from many analytical models (Baber and Wen 1981, Yar and Hammond 1986), the modified Takeda model logically defines the nonlinear hysteretic behavior of RC members.

For the identification of practical structural dynamic systems, it is necessary to reduce the problem size for the efficiency and stability of the identification procedure. The mode superposition method has been extended to the nonlinear dynamic systems for this purpose (Mohraz, *et al.* 1991, Villaverde and Hanna 1992, Aprile *et al.* 1994), and there are several general purpose computer software packages using the mode superposition method for the nonlinear dynamic analysis, such as SAP2000 (Wilson 2002). In spite of the numerical efficiency of this method, however, enough modes have to be included or the truncated mode effects have to be corrected to achieve reasonable accuracy particularly on local behavior (Dikens, *et al.* 1997).

The extended Kalman filter (EKF) has been widely used for the parameter estimation of a nonlinear structural dynamic system. Nonetheless, when the EKF is applied to a complex system or a practically large structural system, a few implementation and numerical problems may arise. To overcome the numerical difficulties in obtaining the state transition matrix, a modified extended Kalman filter (MEKF) was developed (Schei 1997), in which a finite difference scheme is employed to calculate the state transition matrix without explicit calculation of the Jacobian matrix (Nørgaard, *et al.* 2000). However divergence problems related to the system complexity and size and the system/measurement noises still remain in practical applications of the MEKF.

In this study, identification of the nonlinear hysteric behavior of a RC bridge pier subjected to earthquake loads is carried out. Only the acceleration measurements of the input earthquake motion and bridge responses are utilized, which are the easiest quantities in dynamic measurements, particularly for bridges with long-spans. The modified Takeda model is used to describe the hysteretic behavior of the RC member with a small number of parameters, in which nonlinear behavior is described in logical forms rather than an analytical expression. Hence, the modified extended Kalman filter is employed to construct the state transition matrix using a finite difference scheme. A two-step approach so called the sequential modified extended Kalman filter (SMEKF) algorithm is proposed to identify the unknown parameters and the state vector separately in two steps, so that the size of the problem for each identification procedure may be reduced and possible numerical problems may be avoided (Yang, *et al.* 2006, Yang and Huang 2007). Mode superposition with a modal sorting technique is also proposed to reduce the size of the identification problem for the nonlinear dynamic system. Example analyses are carried out for a continuous bridge model with a RC pier subjected to earthquake loads in the longitudinal and transverse directions.

## 2. Nonlinear hysteric behavior of RC bridge piers

Experimental studies have shown that the hysteretic behavior of RC components is dependent upon numerous structural parameters which greatly affect the deformation and energy absorbing characteristics of the components (Park, *et al.* 1972, Otani and Sozen 1972, Atalay and Pezzen 1975). It is, therefore, important to recognize that a highly versatile model is required to closely reproduce the hysteretic behavior, in which several important aspects of hysteretic loops can be included, viz., stiffness degradation, strength deterioration, pinching behavior, and variability of hysteretic areas at different deformation levels under repeated load reversals (Kunnath, *et al.* 1988). However, the model should also be simple to implement.

The modified Takeda model by Roufaiel and Meyer (1987) can effectively describe the nonlinear hysteretic behavior of damaged RC members with a small number of nonlinear parameters. This model allows a finite plastic zone instead of a plastic hinge of zero length, which often leads to too conservative estimates of the rotational ductility capacity of the end section (Mork 1994).

In this study, the modified Takeda model with axial force effect is employed for identification of the nonlinear hysteretic behavior of a RC bridge pier subjected to earthquake excitation. Then the nonlinear parameters in this model are estimated based on the measured acceleration records of the ground motion and structural responses using a Kalman filtering technique; namely the sequential modified extended Kalman filter.

### 2.1. Moment-curvature curve for cyclic loading by the modified Takeda model

Under load reversals, the stiffness of a RC section may experience degradation due to the cracking of the concrete and slip of the reinforcing bar. In the modified Takeda model, four different kinds of branches may exist in the hysteresis of the moment-curvature ( $M-\phi$ ) relationship as in Fig. 2, and each branch is logically defined as

- Elastic loading and unloading of the primary  $M-\phi$  curves are characterized by a slope  $(EI)_1=(EI)_e$ , where  $(EI)_e$  is the elastic stiffness of the RC member.
- Inelastic loading of the primary  $M-\phi$  curve after yield point  $(\phi_y, M_y)$  is defined by a slope

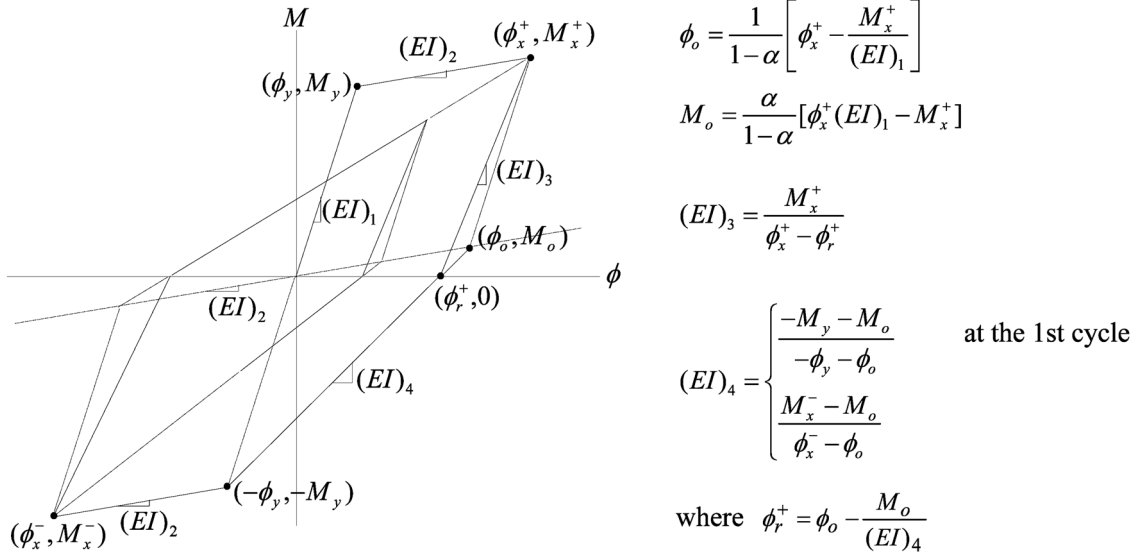


Fig. 2 Hysteretic moment - curvature behavior of the modified Takeda model

$(EI)_2 = \alpha(EI)_e$ , where  $\phi_y$  and  $M_y$  are the yield curvature and yield moment, and  $\alpha$  is the ratio of the post yield stiffness to the elastic stiffness of the RC member.

- Inelastic unloading is defined by a slope  $(EI)_3$ , where two points  $(\phi_o, M_o)$  and  $(\phi_r^+, 0)$  are defined in Fig. 2.

- Inelastic reloading in the negative direction is characterized by a slope  $(EI)_4$ , which may be determined as in Fig. 2.

In Fig. 2,  $(\phi_x^+, M_x^+)$  and  $(\phi_x^-, M_x^-)$  are the maximum previous excursions in the positive and negative directions, which are to be updated along with  $(EI)_3$  and  $(EI)_4$  as the hysteresis proceeds.

## 2.2. Stiffness degradation

Under the load reversals well into the inelastic range, the stiffness of a reinforced concrete member decreases due to the cracking in concrete and slip of reinforced bars. As a consequence, a reduction in the overall structural stiffness occurs. This degradation process is simulated as in Fig. 3(a).

## 2.3. Pinching effect by shear force

From various test data, it was reported that a strong correlation exists between the degree of pinching and the relative magnitude of shear at the section under consideration (Ma, *et al.* 1976, Popov, *et al.* 1972). To reflect the pinching effect into a hysteretic moment-curvature relation representing the bending behavior, Roufaiel and Meyer (1987) proposed a modification of the reloading branch as shown in Fig. 3(b). The characteristic point  $(\phi_p, M_p)$  on the original elastic loading curve is determined as

$$\phi_p = \varepsilon \phi_n; M_p = \varepsilon M_n \quad (1)$$

where  $\varepsilon = 0$  for  $a/d < 1.5$ ,  $\varepsilon = 0.4(a/d) - 0.6$  for  $1.5 < (a/d) < 4.0$ ,  $\varepsilon = 1$  for  $(a/d) \geq 4.0$ ;  $a$  = the shear span

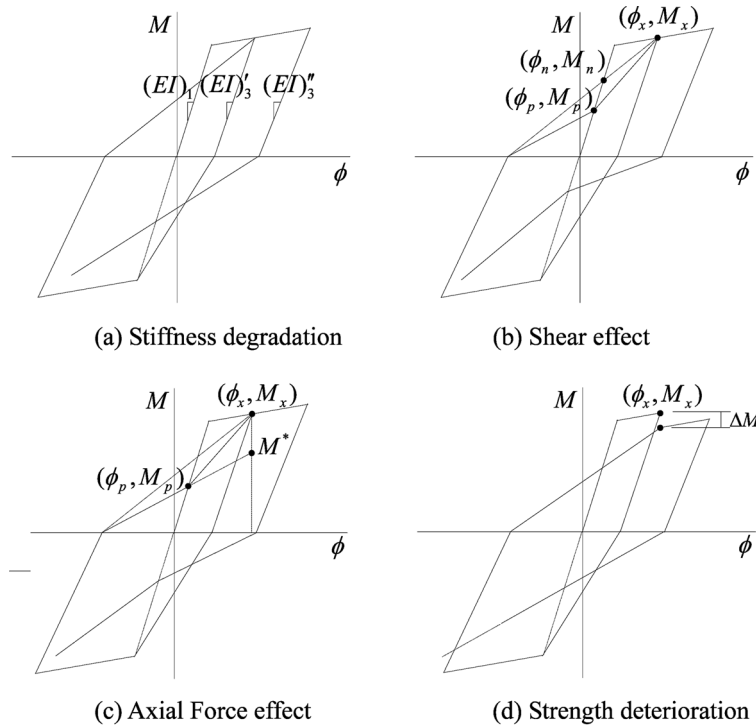


Fig. 3 Significant hysteretic behavior of a RC member

length;  $d$ =the effective depth of the section; and  $(\phi_n, M_n)$  is the crossing pint of the reloading curve and the initial elastic loading curve.

#### 2.4. Pinching effect by axial force

When RC member is subjected to an axial load, the moment-curvature relation may alter. From the empirical formula (Ozcebe and Saatcioglu 1989), which reflects the effect of the axial load on the pinching effect, the following formula was adapted for  $M^*$  in Fig. 3(c) as

$$M^* = M_x \cdot \exp\left(\beta \frac{\phi_x}{\phi_y} \frac{P}{|P_0|}\right) \quad (2)$$

where  $(\phi_x, M_x)$  represents the maximum previous excursion in the opposite direction; the characteristic point  $(\phi_p, M_p)$  can be determined similarly to the case of the shear effect;  $\phi_y$  is the corresponding curvature at yield;  $P$  is the axial compressive force(negative value);  $P_0$  is the nominal compressive strength of the member; and  $\beta$  is the parameter which controls the pinching behavior by the axial force.

#### 2.5. Strength deterioration

If a RC member is strained beyond a certain critical level during cyclic loadings, its strength may deteriorate as shown in Fig. 3(d). The strength deterioration is initiated as soon as the yield load level is exceeded, and the strength deterioration accelerates as the critical load level is reached. The following strength drop index is used, which was proposed by Chung, *et al.* (1989).

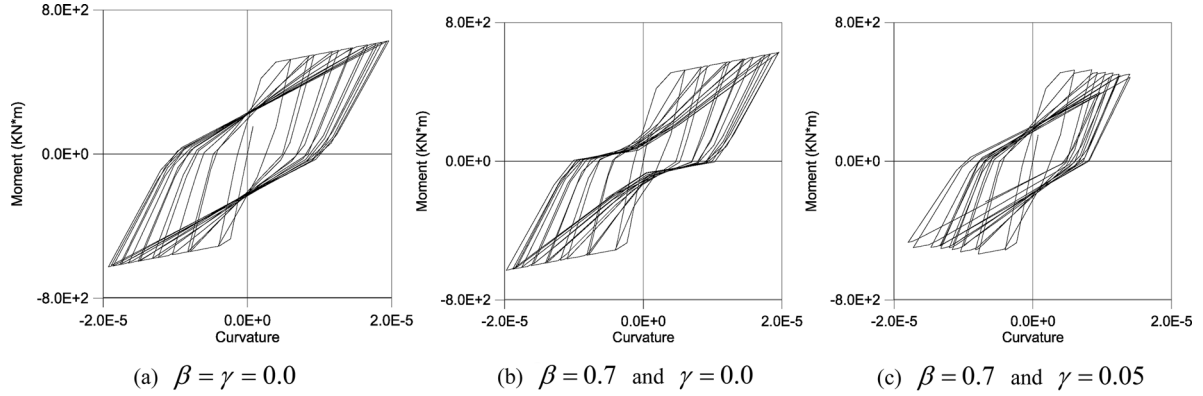


Fig. 4  $M$ - $\phi$  relationships in a RC bridge pier ( $P/|P_o| = 0.2$ ,  $M_y = 500$  kN·m, and  $\alpha = 0.03$ )

$$\frac{\Delta M}{\Delta M_f} = \left( \frac{\phi - \phi_y}{\phi_f - \phi_y} \right)^\omega \quad (3)$$

where  $\Delta M$  is the moment capacity reduction in a single load cycle up to curvature  $\phi$ , and  $\Delta M_f$  is the fictitious moment capacity reduction in a single load cycle up to failure curvature  $\phi_f$ . For parameter  $\omega$ , calibration studies suggested a value of 1.5. If the strength deterioration parameter  $\gamma$  is introduced, and  $\Delta M_f = C_1 M_y$ ,  $\phi_f = C_2 \phi_y$ , and  $\phi = \phi_x$ , where  $C_1$  and  $C_2$  are constant, Eq. (3) can be rewritten as

$$\Delta M = \gamma M_y \left( \frac{\phi_x - \phi_y}{\phi_y} \right)^{1.5} \quad (4)$$

Fig. 4 shows typical hysteretic behavior of a RC pier subjected to cyclic loadings for several cases of parameters  $\beta$  and  $\gamma$ .

### 3. Nonlinear dynamic analysis by mode superposition with modal sorting

In this study, the concrete bridge pier is assumed to be locally damaged at the bottom of the pier due to severe earthquake ground motion. It is also assumed that dominant nonlinear hysteretic behaviors such as stiffness degradation, pinching, and stiffness deterioration can be effectively represented by the Modified Takeda model with 4 parameters  $M_y$ ,  $\alpha$ ,  $\beta$  and  $\gamma$  described in Section 2.

Nonlinear dynamic analysis is generally carried out by means of a direct step-by-step integration, which involves a large number of degrees of freedom (DOFs) and high computational cost. However, a dynamic formulation with a large number of DOFs may cause serious difficulty in the present nonlinear system identification problem. Hence modal superposition with a modal sorting scheme is employed in approximation in the nonlinear dynamic analysis procedure, so that the size of the identification problem may be reduced and the efficiency and accuracy of the parameter identification may be improved.

#### 3.1. Nonlinear equation of motion

If a structure is subjected to a severe earthquake load, some weak elements may experience damage and the dynamic response of the structural system becomes nonlinear, which can be generally described

by a nonlinear equation of motion as

$$M\ddot{U}(t) + C\dot{U}(t) + KU(t) + R(t) = -M\{L\}\ddot{u}_g(t) \quad (5)$$

where  $M$ ,  $C$  and  $K$  are the mass, damping, and initial stiffness matrix;  $U(t)$ ,  $\dot{U}(t)$ ,  $\ddot{U}(t)$  are the displacement, velocity, and acceleration vectors;  $\{L\}$  is the influence vector accounting the direction of the earthquake excitation;  $\ddot{u}_g(t)$  is the ground acceleration, and  $R(t)$  is the nonlinear residual force vector.

Then Eq. (5) can be rewritten as

$$M\ddot{U}(t) + C\dot{U}(t) + KU(t) = \bar{R}(t) \quad (6)$$

where  $\bar{R}(t) = -M\{L\}\ddot{u}_g(t) - R(t)$

### 3.2. Mode superposition method with modal sorting

A mode superposition method is used in approximation to reduce the size of the present nonlinear dynamic problem, and the diagonal modal damping is assumed in this study. Then a series of modal equations of motion can be obtained from Eq. (6) as

$$\ddot{q}_n(t) + 2\zeta_n\omega_n\dot{q}_n(t) + \omega_n^2q_n(t) = \bar{f}_n(t) \quad (n=1, 2, \dots, l) \quad (7)$$

where  $q_n(t)$ ,  $\dot{q}_n(t)$  and  $\ddot{q}_n(t)$  are the modal displacement, velocity and acceleration for the  $n$ -th mode;  $\zeta_n$  and  $\omega_n$  are the corresponding damping ratio and natural frequency; and  $\bar{f}_n(t)$  is the modal load which includes the nonlinear residual force which depends on the unknown concurrent structural response. Hence, the above modal equations can be solved iteratively at each time by updating the nonlinear residual force.

From Eq. (7), the following discrete dynamic equation may be obtained at  $t = k\Delta t$ :

$$\begin{aligned} \begin{Bmatrix} q_n \\ \dot{q}_n \\ \ddot{q}_n \end{Bmatrix}_{k+1} &= [A] \begin{Bmatrix} q_n \\ \dot{q}_n \\ \ddot{q}_n \end{Bmatrix}_k + [B] \{ \bar{f}_n(t; q_n, \dot{q}_n, \ddot{q}_n) \} \\ &= g(q_n(k), \dot{q}_n(k), \ddot{q}_n(k), \bar{f}_n(t; q_n, \dot{q}_n, \ddot{q}_n)) \end{aligned} \quad (8)$$

where  $[A]$  and  $[B]$  are constant matrices which may be obtained using the Wilson- $\theta$  method, and  $g(\cdot)$  is a function of the state transition.

When the mode superposition method is applied for the analysis of the dynamic systems, the truncation of modes may cause significant difficulty in obtaining reasonable dynamic response (D'Aveni and Muscolino 2001), particularly for the locally damaged behavior, which is directly related to the system identification. Therefore, a modal sorting technique is proposed to select the modes with larger contribution to the DOF near the damaged location. The  $j$ -th modal contribution to the  $i$ -th DOF  $\Xi_{ij}$  under earthquake load may be evaluated as

$$\Xi_{ij} = \phi_{ij}\Gamma_jS_j \quad (9)$$

where  $\phi_{ij}$  is the  $j$ -th eigenvector at the  $i$ -th DOF,  $\Gamma_j$  is the modal participation factor at the  $j$ -th mode;  $S_j$  is the deformation response spectrum of the ground motion at the  $j$ -th natural period at  $\omega = \omega_j$ . The modes are sorted by the order of the magnitudes of those modal contribution values for a specific DOF. With the sorted modal vectors, the global displacement vector can be obtained as

$$U(t) = \tilde{\Phi}Q(t) \quad (10)$$

where  $\tilde{\Phi}$  is the matrix of the sorted eigen-vectors matrix, and  $Q(t)$  is the corresponding modal displacement vector.

#### 4. Identification of nonlinear parameters by extended Kalman filtering techniques

##### 4.1. State equation

For identifying the hysteretic behavior of a RC bridge pier under severe earthquake loads, the extended Kalman filtering (EKF) technique is utilized in this study. At first a series of the modal equations of motion in discrete time, Eq. (8), are transformed into a general form of a nonlinear discrete state equation at  $t = k\Delta t$  as

$$X_{k+1} = G(X_k, \bar{f}_k(X_k); k) + w_k \quad (11)$$

where  $X_k$  is the augmented state vector including the modal displacements, velocities, accelerations and the unknown parameters ( $M_y$ ,  $\alpha$ ,  $\beta$  and  $\gamma$  as defined in Section 2) as

$$X_k = [q_1(k) \quad \dot{q}_1(k) \quad \ddot{q}_1(k) \quad \dots \quad q_l(k) \quad \dot{q}_l(k) \quad \ddot{q}_l(k) \quad M_y(k) \quad \alpha(k) \quad \beta(k) \quad \gamma(k)^T] \quad (12)$$

where  $l$  is the number of modes included; and  $w_k$  is a system noise vector with a covariance  $Q$ . In Eq. (12), the unknown parameters are treated as time varying quantities, so their estimates may be updated as the time progresses.

In Eqs. (11)-(12) the state vector includes the acceleration terms in addition to the conventional state vector consisting of displacement and velocity terms. Eq. (11) is obtained using the Wilson- $\theta$  method with  $\theta=1.4$  for each modal equation of motion. Acceleration records are easier to measure than displacement and velocity, particularly for bridges with long-spans, hence only acceleration measurements are utilized in the present identification problem. Then the observation equation can be written as

$$Y_k = H_k X_k + v_k \quad (13)$$

where

$$H_k = \begin{bmatrix} 0 & 0 & \phi_{i1} & 0 & 0 & \phi_{i2} & \dots & 0 & 0 & \phi_{il} & 0 & 0 & 0 & 0 \\ 0 & 0 & \phi_{j1} & 0 & 0 & \phi_{j2} & \dots & 0 & 0 & \phi_{jl} & 0 & 0 & 0 & 0 \\ & & & & & & \vdots & & & & & & & \\ 0 & 0 & \phi_{m1} & 0 & 0 & \phi_{m2} & \dots & 0 & 0 & \phi_{ml} & 0 & 0 & 0 & 0 \end{bmatrix} \quad (14)$$

and  $Y_k$  is the acceleration measurement vector at  $t = k\Delta t$ , which contains the relative accelerations at the

selected nodes to the ground motion that can be obtained by subtracting the measured ground acceleration from the measured absolute accelerations of the structure;  $H_k$  is the observation matrix;  $\phi_{ij}$  are the  $i$ -th DOF component of the  $j$ -th mode selected by the modal sorting;  $i, j, \dots$ , and  $m$  are the measured DOFs; and  $v_k$  is the observation noise vector with a covariance  $R_k$ .

#### 4.2. Extended Kalman filter

The extended Kalman filter (EKF) is used for the sequential state estimation based upon the observed data of the response. At a time step  $k$ , the state  $X_{k+1}$  and the error covariance matrix  $P_{k+1|k}$  for the next time step  $k+1$  can be predicted by using the discrete state equation, Eq. (11), as

$$\hat{X}_{k+1|k} = G(\hat{X}_{k|k}, \bar{f}_k) \quad (15)$$

$$P_{k+1|k} = \Phi_{k+1|k} P_{k|k} \Phi_{k+1|k}^T + Q_k \quad (16)$$

where  $\Phi_{k+1|k}$  is the state transition matrix which can be approximately obtained using the Jacobian matrix as

$$\Phi_{k+1|k} = I + \Delta t \left. \frac{\partial G(X, f; t)}{\partial X} \right|_{X = \hat{X}_{k|k}} \quad (17)$$

and the covariance of the system noise  $Q_k$  is commonly taken as a time-invariant value.

As the observation  $Y_{k+1}$  becomes available at  $k+1$ , the state vector and the error covariance can be updated by a filtering process as (Yun and Shinozuka 1980, Hoshiya and Sato 1984).

$$\hat{X}_{k+1|k+1} = \hat{X}_{k+1|k} + K_{k+1} [Y_{k+1} - H_{k+1} \hat{X}_{k+1|k}] \quad (18)$$

$$P_{k+1|k+1} = [1 - K_{k+1} H_{k+1}] P_{k+1|k} [1 - K_{k+1} H_{k+1}]^T + K_{k+1} R_k K_{k+1}^T \quad (19)$$

where  $K_{k+1}$  is the Kalman gain matrix at time step  $k+1$  as

$$K_{k+1} = P_{k+1|k} H_{k+1}^T [H_{k+1} P_{k+1|k} H_{k+1}^T + R_k]^{-1} \quad (20)$$

and the covariance of the observation noise  $R_k$  is also taken as a time-invariant value.

Then the prediction of the state may proceed to the next time step  $k+2$ .

#### 4.3. Modified extended Kalman filter

The EKF is based on the first order Taylor approximation of the state transition equation on the estimated state trajectory. However, there are limitations if the first order derivatives of the nonlinear terms are not well defined as in the modified Takeda model used in the present study, so that the covariance matrices in Eq. (15) may not be adequately evaluated. Schei (1997) proposed the modified extended Kalman filter (MEKF) algorithm with a finite difference scheme to improve this limitation of the EKF.

In the MEKF, the state transition matrix is approximately obtained using a finite difference scheme as

$$\Phi_{k+1|k} = \left[ \frac{\partial G_i(X)}{\partial X_j} \right] \approx \frac{1}{2e_j} [G_i(X+e_j) - G_i(X-e_j)] \quad (21)$$

where  $e_j$  is small perturbation in the  $j$ -th component of the state vector  $X$ . Using this state transition matrix and Cholesky factorization of the error covariance matrixes  $P_{k/k}$ , the predicted error covariance  $P_{k+1/k}$  at time step  $k+1$  can be obtained without calculation of the Jacobian matrix in Eq. (17). The square root estimation procedure has been utilized for keeping the positive definiteness of the error covariance matrix (Schei 1997). Then the updated state vector and covariance matrix  $\hat{X}_{k+1|k+1}$  and  $P_{k+1|k+1}$  can be obtained using the same procedure of the EKF.

#### 4.4. Sequential modified extended kalman filter

In the EKF and MEKF techniques, an augmented state vector including the unknown parameters is used for the identification of the parameters. Therefore the size of the state vector and the corresponding state equation can be easily too big to handle particularly for the problems related to real and practical structural systems. Hence, in this study, two steps approach so called the sequential modified extended Kalman filter (SMEKF) is proposed. At first the state vector consisting of only the system responses is estimated based on the concurrent estimates of the parameters using the MEKF. Then the unknown parameters are identified based on the estimated state using the sequential prediction error method (Goodwin and Sin 1984, Lee and Yun 1991, Yun, *et al.* 1997, Blumin and Pogodaev 2003). The SMEKF procedure is summarized in Fig. 5.

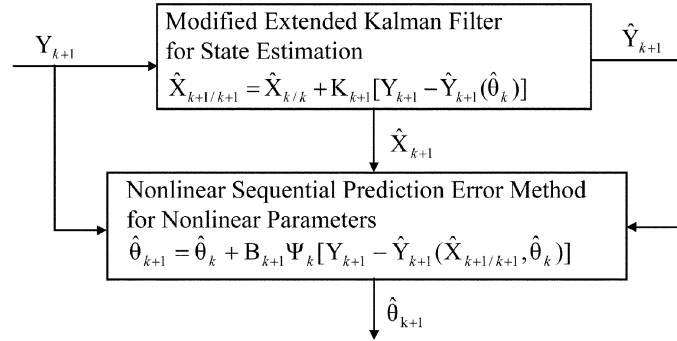


Fig. 5 Sequential modified extended kalman filter (SMEKF) algorithm

The sequential prediction error method for the parameter estimation can be summarized as

$$\hat{\theta}_{k+1} = \hat{\theta}_k + B_{k+1} \Psi_k \{e(k+1, \hat{\theta}_k)\} \quad (22)$$

where  $e(k+1, \hat{\theta}_k) = Y_{k+1} - H_{k+1} \hat{X}_{k+1|k+1}(\hat{\theta}_k)$ ; and  $B_{k+1}$  is the adaptation gain matrix which can be obtained as

$$B_{k+1}^{-1} = B_k^{-1} + \Psi_k \Psi_k^T \quad (23)$$

and  $\Psi_k$  is the Jacobian matrix of the observation error vector function  $e(k+1, \hat{\theta}_k)$  as

$$\Psi_k = -\left. \frac{\partial e(k+1, \theta)}{\partial \theta} \right|_{\theta = \hat{\theta}_k} \quad (24)$$

In Eq. (22),  $\Psi_k$  is approximately evaluated using a finite difference scheme similarly to the state transition matrix  $\Phi_{k+1/k}$ . Then Eq. (22) can be rewritten as

$$\hat{\theta}_{k+1} = \hat{\theta}_k + L_{k+1}^T E_k \{e(k+1, \hat{\theta}_k)\} \quad (25)$$

where  $L_{k+1}$  is the Cholesky decomposition of the adaptation gain matrix  $B_{k+1}$ , and

$$(E_{ij})_k = \left. \frac{e_i(\theta + l_j) - e_i(\theta - l_j)}{2} \right|_{\theta = \hat{\theta}_k} \quad (26)$$

and  $l_j$  is the  $j$ -th row vector of the Cholesky-decomposed adaptation gain matrix. The updated adaptation gain matrix in Eq. (23) maintains the positive definiteness by using the square root estimation scheme (Schei 1997).

In general large initial values of the error covariance  $P_{0/0}$  and the adaptation gain matrix  $B_0$  increase the speed of convergence, but deteriorate the stability (Loh and Chung 1993). In MEKF and SMEKF, the sensitivities of the identification results to those initial values are found to be increased by introducing the finite difference scheme to the state transition matrix. So, for the stable parameter estimation, it is needed to reduce the time increment of the identification procedure or to carry out global iterations with small values of  $P_{0/0}$  and  $B_0$ . If the adaptive techniques which have been proposed by Sato and Chung (2005), Yang and Lin (2005), and Yang, *et al.* (2006) are applied, the number of required global iteration may be reduced. However, such techniques are not considered in this study.

## 5. Examples for identification of hysteretic behavior of RC piers

### 5.1. Single degree of freedom case

The first example is an idealized single degree of freedom case with a lumped mass and a vertical column, as shown in Fig. 6(a). The lumped mass is 500 ton, and the sectional properties of the column are shown in Fig. 6(a).

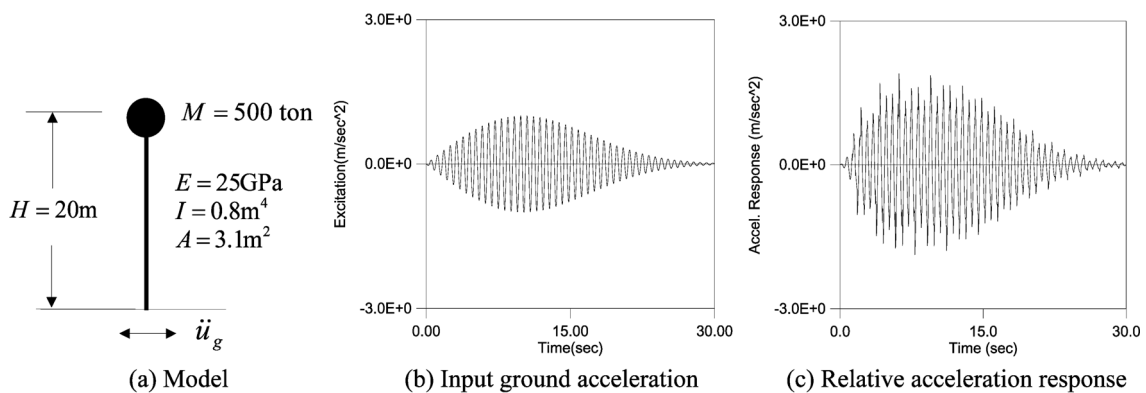


Fig. 6 Single degree of freedom model

The nonlinear hysteretic behavior of the column is examined for a harmonic load with a frequency 1.5 Hz and a slowly varying envelope as shown in Fig. 6(b). The hysteretic behavior is characterized using the modified Takeda model with four nonlinear parameters; i.e.,  $M_y$ ,  $\alpha$ ,  $\beta$  and  $\gamma$  as in Section 2. It is assumed that the shear span to depth ratio ( $a/d$ ) is greater than 4.0, so  $\varepsilon = 1.0$  in Eq. (1). Then the pinching effect is only affected by a constant axial force of  $P/|P_o| = 0.2$  in Eq. (2). The exact values of the nonlinear parameters are assumed as  $M_y = 500 \text{ KN}\cdot\text{m}$ ,  $\alpha = 0.03$ ,  $\beta = 0.7$ , and  $\gamma = 0.02$ . The natural frequency of the undamaged linear case is obtained as 1.39 Hz, and the damping ratio is assumed as 5%. For the nonlinear parameter estimation of this model, the ground motion and acceleration responses are assumed to be measured. Fig. 6(c) shows the relative acceleration response of the lumped mass. The measurement noises are assumed to be 3% of the exact values in the root mean square (RMS) levels.

The acceleration response is included in the state vector in order to use the measured acceleration data directly. The state vector is taken differently for the MEKF and SMEKF methods as

In the MEKF method:  $X = [q \ \dot{q} \ \ddot{q} \ M \ \alpha \ \beta \ \gamma]^T$

In the SMEKF method;  $[X = q \ \dot{q} \ \ddot{q}]^T$  for the state estimation in the MEKF procedure, while  $\theta = [M \ \alpha \ \beta \ \gamma]^T$  for the parameter estimation in the SPEM procedure.

The initial guesses for the nonlinear parameters  $\theta_0$  were taken as the values of 50% of the exact values as shown in Table 1. The initial value of the adaptation gain matrix  $B_0$  and the error covariance matrix  $P_{0/0}$  are customarily taken through trial and error procedures. Generally those values used to be taken as large values to speed up the convergence. Special schemes such as adaptive data weighting are frequently employed to improve the stability and accuracy. In the present study, the initial  $B_0$  was taken as a diagonal matrix with diagonal elements of 2.0, 0.5, 0.1, and 0.01 of the initial values of  $M_y$ ,  $\alpha$ ,  $\beta$  and  $\gamma$ , respectively, and initial  $P_{0/0}$  was taken as the diagonal matrix with 0.01 in the diagonals. Compared with the case using the conventional EKF, those initial values were taken to be relatively small values to secure the stability of the MEKF and SMEKF which use a finite difference scheme, so a considerably larger number of global iterations were required. The values of the system noise covariance matrix  $Q$  and the observational noise covariance matrix  $R$  were also chosen through several trials, because those values affect the accuracy and robustness of identification. The diagonal values of  $R$  are commonly taken as the RMS values of the observational noises. In general a large value of  $R$  improves the robustness of identification, but deteriorates the accuracy. On the other hand, a small value of  $R$  may cause a divergence problem in identification. In this study, the diagonal values of  $R$  and  $Q$  were taken as 0.01.

The time step  $\Delta t$  of each identification step was taken as 0.002 sec, and the parameter estimation was carried for duration of 10 sec. From Table 1 and Figs. 7 and 8, it can be observed that the estimated parameters and hystereses by both of the MEKF and SMEKF methods are very excellent, though the results by the SMEKF are better. It is interesting to note that the acceleration responses recalculated using the identified nonlinear parameters by two methods very well coincide with the exact value as in Figs. 7(b) and 8(b).

Fig. 9 shows the parameter tracking procedures for four nonlinear parameters in global iterations by the SMEKF. For the present hysteretic behavior for a RC pier, the yield moment and post yield stiffness parameters ( $M_y$  and  $\alpha$ ) mainly control the overall shape of the hysteresis, while the remaining parameters ( $\beta$  and  $\gamma$ ) reflect the pinching and strength deterioration characteristics. It has been found that the estimates for the first two parameters ( $M_y$  and  $\alpha$ ) converge to the assumed exact values much faster, while the estimates of the other two parameters ( $\beta$  and  $\gamma$ ) depend on the accuracy of the former two. It is also found from a series of parametric studies that the required number of the global iterations

Table 1 Results of parameter estimations for a SDOF model

Nonlinear Parameters	$M_y$ (KN·m)	$\alpha$	$\beta$	$\gamma$
Exact Values	500.0	0.0300	0.7000	0.0200
Initial guesses	250.0	0.0150	0.3500	0.0100
With SMEKF	504.6	0.0296	0.6967	0.0201
With MEKF	511.2	0.0323	0.6352	0.0158

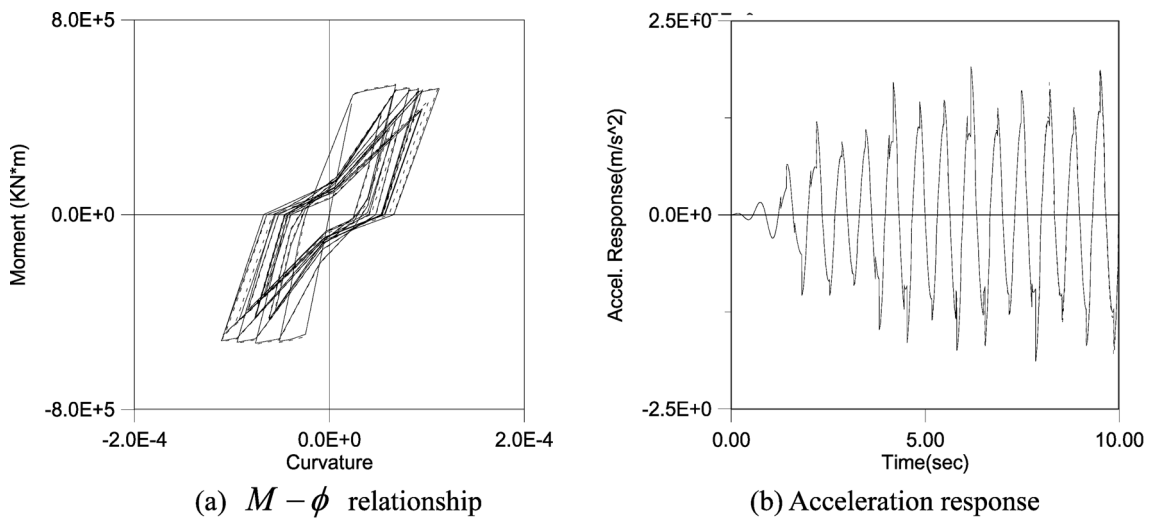


Fig. 7 Nonlinear responses estimated by the SMEKF (—: Exact and ----: Estimated)

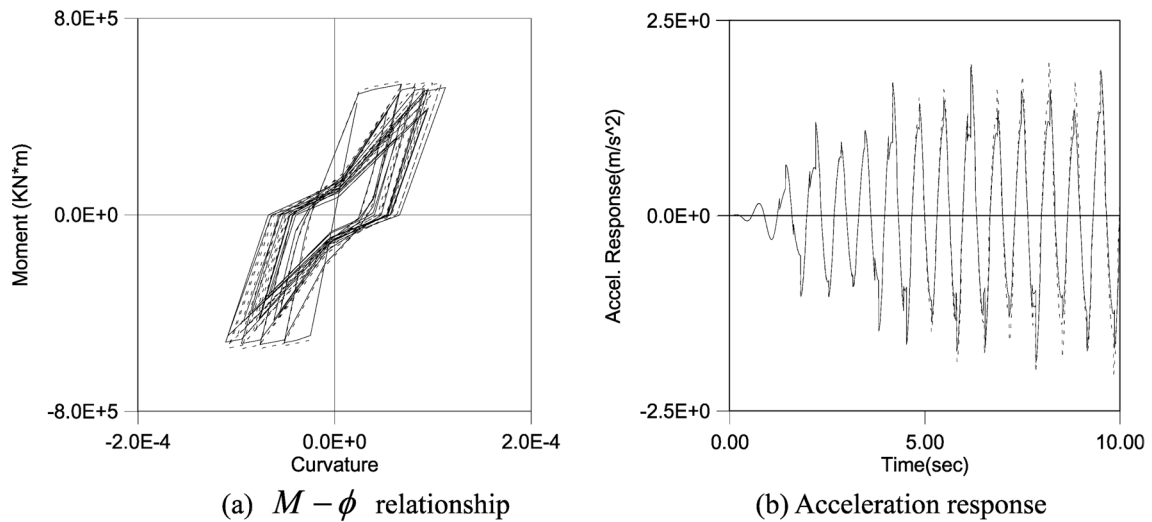


Fig. 8 Nonlinear responses estimated by the MEKF (—: Exact and ----: Estimated)

for the parameter estimation is about 20 for this example, and it may be reduced by reducing the time step for the parameter estimation.

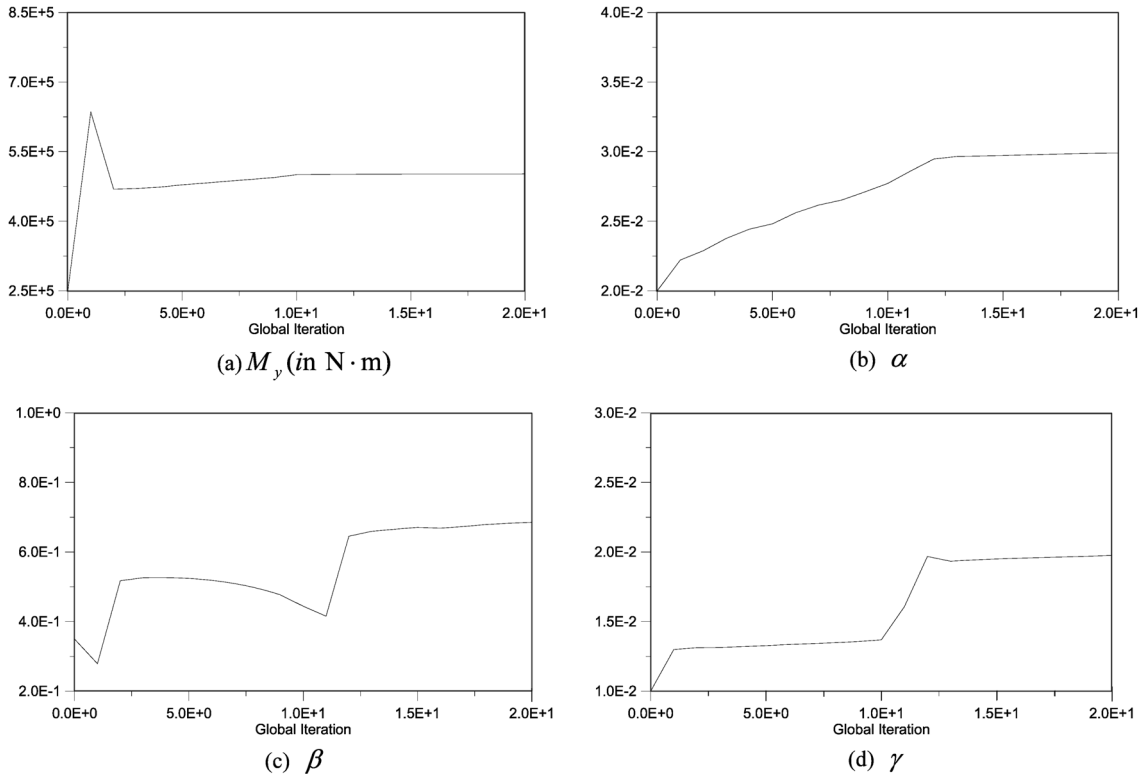


Fig. 9 Parameter tracking procedures in global iterations by the SMEKF

## 5.2. Two-span continuous bridge model in longitudinal direction

The second example is a simplified continuous bridge model with a pier in the middle of the deck. It is assumed that the deck is supported by rollers at both ends in the longitudinal direction of the bridge and earthquake load is applied in the direction, so the effect of the deck may be considered as an additional lumped mass on the top of the pier. The pier is modeled by 5 beam elements in the 2-D plan. Two DOFs; i.e., a longitudinal displacement and a rotation, are assigned at each node, so the total number of DOFs is 10. The geometric and sectional properties of the pier are shown in Fig. 10. A scaled El Centro earthquake (NS, peak ground acceleration (pga)=0.15 g, 1940) is used in this study. Nonlinear hysteretic behavior is assumed to occur at the bottom of the pier during the earthquake.

Fig. 11 shows the measured input earthquake acceleration and relative acceleration response at the top of the pier. The corresponding moment-curvature response at the bottom of the pier is also shown in Fig. 11(c).

The assumed exact values of the parameters of the hysteretic behavior are:  $M_y = 1200$  KN·m,  $\alpha = 0.01$ ,  $\beta = 1.0$ , and  $\gamma = 0.05$ . The first natural frequency of this model in the longitudinal direction is obtained as 0.64 Hz, while the damping ratio is assumed as 5% viscous damping for each mode.

In this example, the performance of two system identification techniques, i.e., the SMEKF and MEKF, is compared, and the influence of the number of the modes included in the nonlinear dynamic analysis is examined. It is assumed that random noises are included in the measured ground excitation and acceleration response at the top of the pier and the noise levels are 3% in RMS levels. The initial

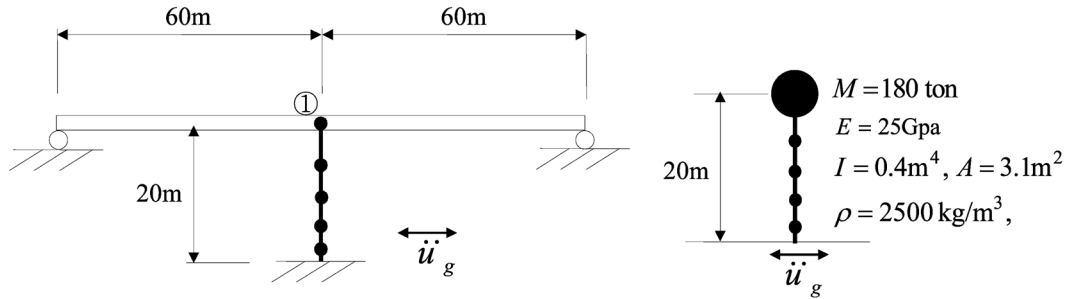


Fig. 10 Two span continuous bridge model subjected earthquake excitation in longitudinal direction

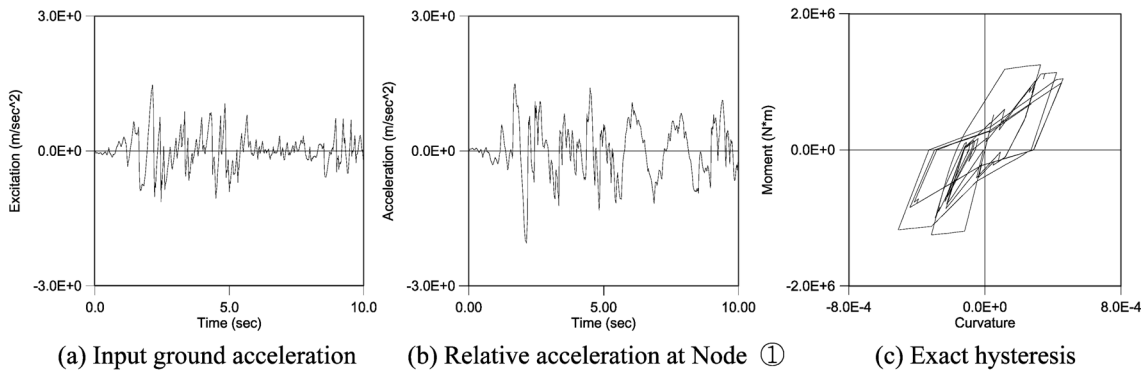


Fig. 11 Input excitation and nonlinear responses

Table 2 Estimated parameters of bridge pier for earthquake in longitudinal direction

Nonlinear Parameters		$M_y$ (KN·m)	$\alpha$	$\beta$	$\gamma$
Exact Values		1200.0	0.0100	1.0000	0.0500
Initial guesses		600.0	0.0050	0.5000	0.0250
w/ 1 mode	SMEKF	849.5	0.0090	1.1373	0.0349
	MEKF	901.3	0.0122	0.5649	0.0421
w/ 3 modes	SMEKF	1175.5	0.0093	1.0876	0.0352
	MEKF	892.9	0.0122	1.6470	0.0345

guesses for the nonlinear parameters  $\theta_0$  were taken as the values of 50% of the exact values as shown in Table 2. The initial adaptation gain matrix  $B_0$  was taken as a diagonal matrix with diagonal elements of 2.0, 0.5, 0.01 and 0.001 of the initial values of  $M_y$ ,  $\alpha$ ,  $\beta$ , and  $\gamma$ , respectively, through several trials. The initial error covariance matrix  $P_{0/0}$  and the system and observation noise covariance matrices  $Q$  and  $R$  were taken as diagonal matrices with 0.01 in the diagonals as in the previous example.

Table 2 and Figs. 12 and 13 show that the SMEKF has provided excellent estimates for the nonlinear parameters with the acceleration response measurement only at the top of the pier, if the first 3 modes are used in the dynamic analysis. On the other hand, the MEKF has failed to give reasonable estimates for the present system of multi-degrees of freedom with a very limited observation data.

In the nonlinear system identification using the mode superposition, if more modes are introduced, more accurate results can be obtained. As shown in Fig. 12, the accuracy in the identification improves with the increasing number of the modes (i.e. 3 modes) used in the SMEKF. But the estimated results

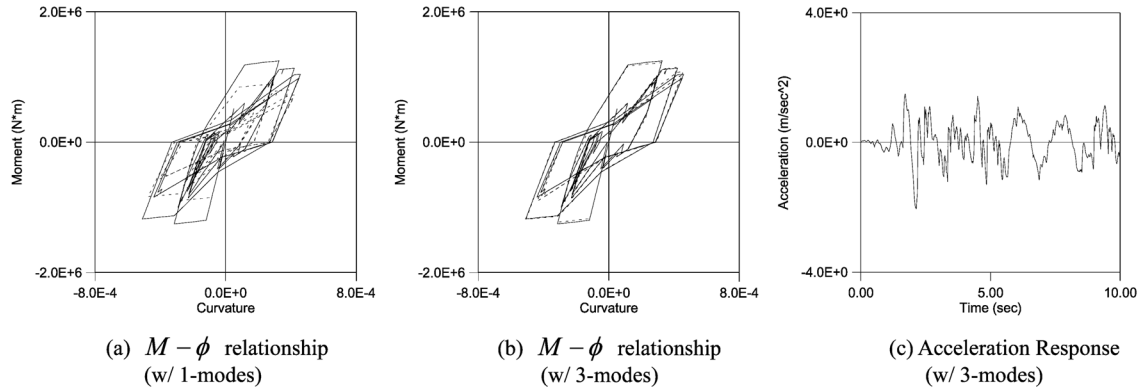


Fig. 12 Recalculated hysteretic relationships and acceleration response using the estimates by the SMEKF and modal sorting (—: Exact and - - - -: Estimated)

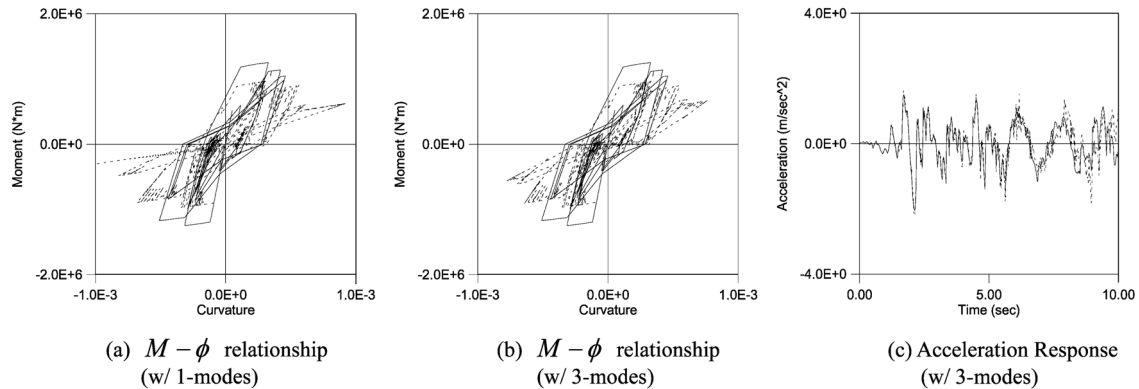


Fig. 13 Recalculated hysteretic relationships and acceleration response using the estimates by the MEKF and modal sorting (—: Exact and - - - -: Estimated)

by the MEKF do not improve even though 3 modes are included. This is due to the increased system dimension and complexity in the augmented state vector used in the MEKF, particularly for the present complex hysteretic behavior. The results also show the limitation of the MEKF for multi-degrees of freedom with a very limited number of the observation response; i.e. one acceleration measurement at the top of the pier. The recalculated acceleration responses at the top of the pier using the identified nonlinear parameters are compared with the exact value in Figs. 12(c) and 13(c). The response recalculated using the identified nonlinear parameters by the SMEKF have been found to coincide very well with the exact value.

### 5.3. Two-span continuous bridge model in transverse direction

The third example is a two span continuous bridge model subjected to an earthquake load in the transverse direction. The bridge deck has hinge supports at both ends in the transverse direction. It is assumed that the deck and the pier have uniform cross-sections. The bridge structure is modeled by beam elements; 10 elements for the deck and 5 elements for the pier as in Fig. 14. The bottom of the bridge pier is assumed to be damaged by a scaled El Centro earthquake (NS,  $p_{ga} = 0.4 g$ , 1940). The

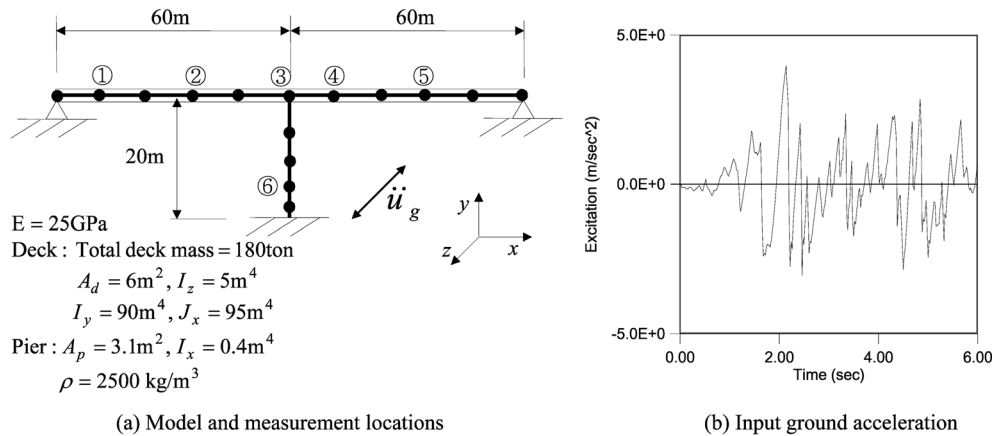
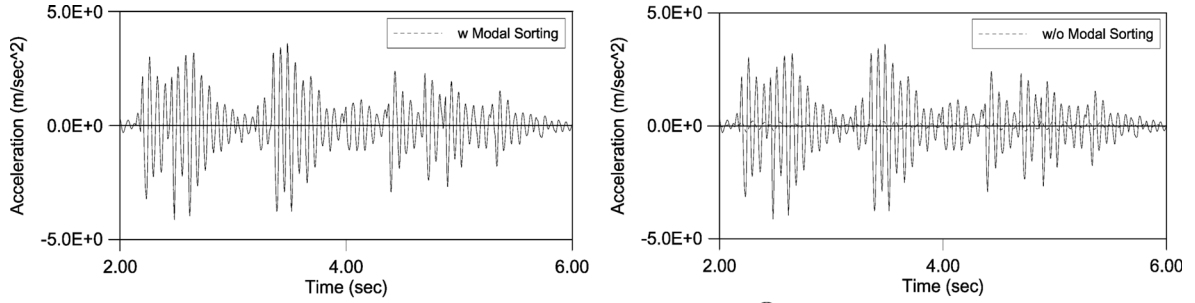


Fig. 14 Two span continuous bridge model and input ground motion in the transverse direction

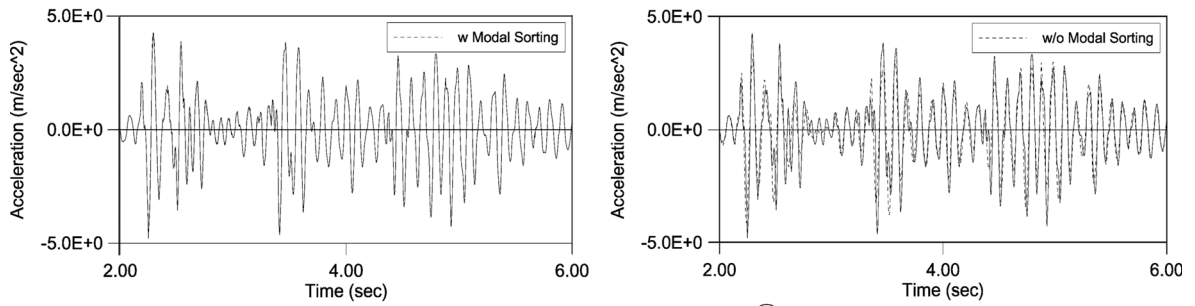
geometric and sectional properties are shown in Fig. 14(a). Since the present example structure is symmetric with respect to the bridge pier, the response in the transverse direction may be calculated by assigning 2 DOFs at each node; i.e., a transverse displacement and a rotation. However, in this example, 6 DOFs were assigned at each node to demonstrate the effectiveness of the modal sorting approach. The acceleration responses in the transverse direction are assumed to be measured at 6 points, 5 points on the bridge deck and 1 point near the bottom of the pier, as shown in Fig. 14(a). It is assumed that 3% noises in RMS level are included in the excitation and response measurements. The input ground acceleration is shown in Fig. 14(b). The nonlinear parameters of the hysteretic behavior at the bottom of the pier are assumed as  $M_y = 1200 \text{ KN}\cdot\text{m}$ ,  $\alpha = 0.01$ ,  $\beta = 1.0$ , and  $\gamma = 0.2$ . The fundamental natural frequency of this bridge model is obtained as 6.31 Hz in the vertical direction and 9.3 Hz in the transverse direction (the 3<sup>rd</sup> mode). The viscous damping ratio is assumed as 5% for each mode.

In this example, mode superposition with modal sorting is utilized to reduce the problem size for the system identification. To evaluate the performance of the proposed modal sorting method, modal contribution values in Eq. (9) were estimated at Node ⑥ near the bottom of the bridge pier in Fig. 14, in which local damage was expected during the earthquake. In the present case with a deck and a pier, two lowest modes are the vertical modes of the deck, so they do not contribute any to the bridge response for the earthquake load in the transverse direction. That is why the modal sorting has been introduced here. Fig. 15 shows the effectiveness of the modal sorting method in the nonlinear dynamic analysis. It is noteworthy that all the modes selected by the modal sorting method are transversely dominant modes. Hence the transverse responses of the pier computed using the first 5 sorted modes are found to be very reasonable. However, those without using the modal sorting scheme gave erroneous estimates owing to the omission of important modes in the direction. The results also show that practically exact dynamic responses can be obtained using 12 modes either sorted or unsorted. Fig. 16 shows that the nonlinear  $M-\phi$  curves can be exactly reproduced using 12 sorted modes.

The initial guesses for the nonlinear parameters  $\theta_0$  were taken as the values of 50% of the exact values. The initial adaptation gain matrix  $B_0$  was taken as a diagonal matrix with diagonal elements of 2.0, 0.5, 0.01 and 0.001 of the initial values of  $M_y$ ,  $\alpha$ ,  $\beta$ , and  $\gamma$ , respectively. The initial error covariance

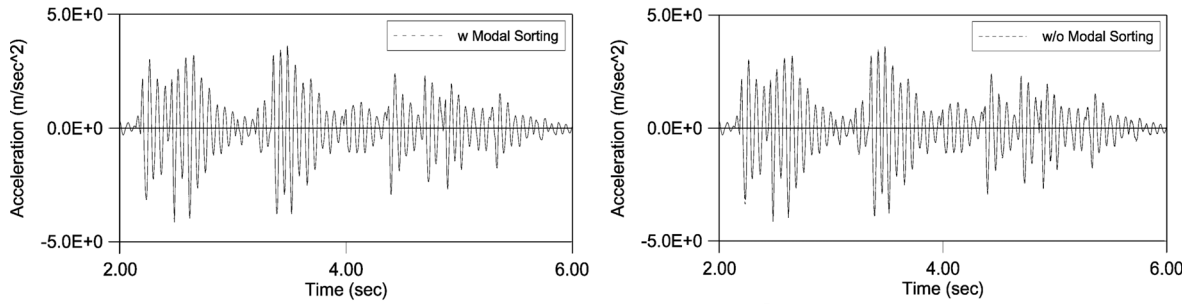


Acceleration responses at Node ③

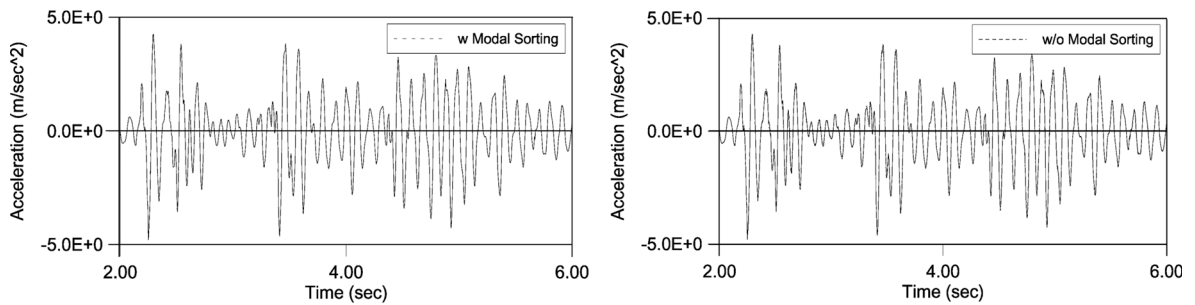


Acceleration responses at Node ⑥

(a) with 5 modes (included modes by modal sorting: 3, 6, 11, 14, 15)



Acceleration responses at Node ③



Acceleration responses at Node ⑥

(b) with 12 modes (included modes by modal sorting: 3, 6, 11, 14, 15, 17, 18, 20, 22, 26, 30)

Fig. 15 Acceleration responses by mode superposition with modal sorting (2-6 sec; : Exact and : Recalculated)

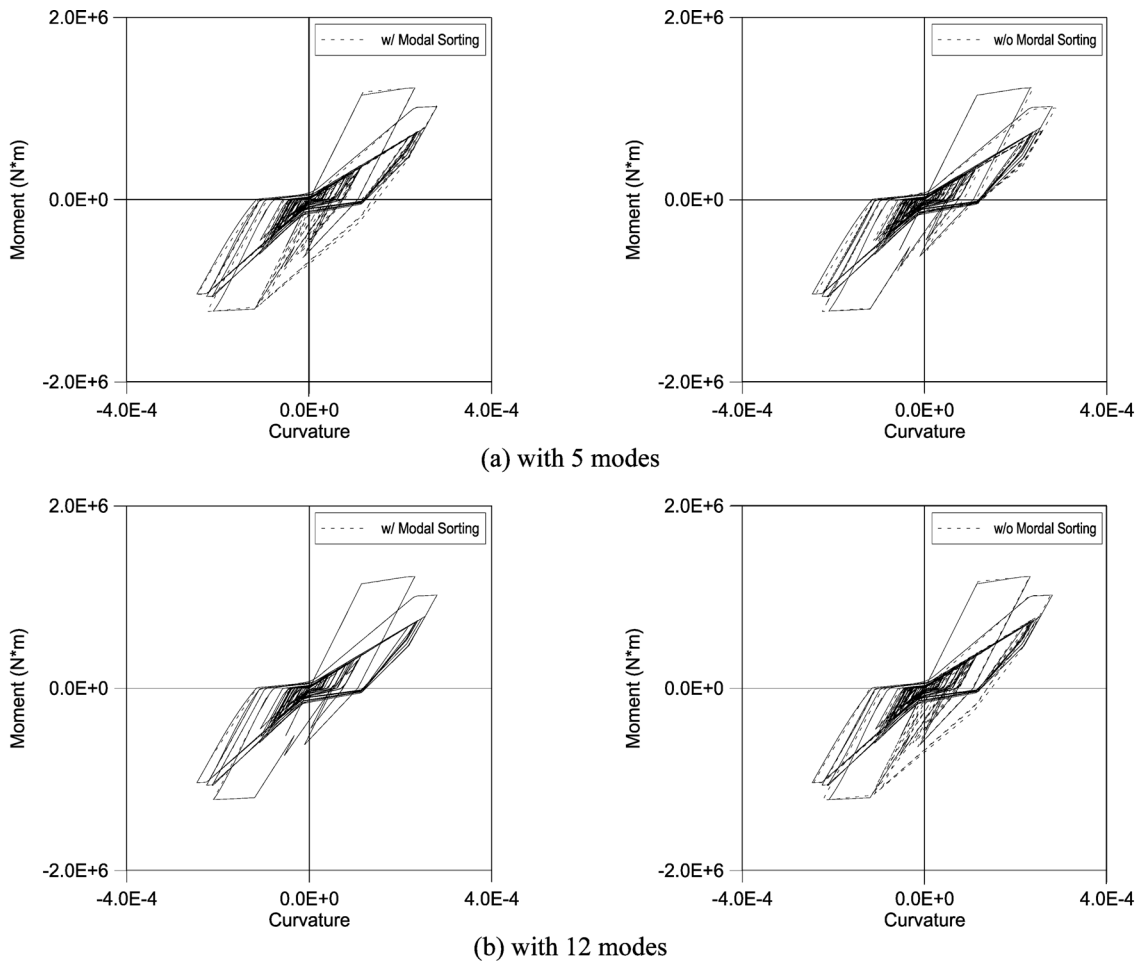


Fig. 16  $M-\phi$  relationships by mode superposition with or without modal sorting using the exact parameters (—: Exact and ----: Recalculated)

Table 3 Estimated parameters of bridge pier in transverse direction using modal sorting and SMEKF

Nonlinear Parameters	$M_y$ (KN·m)	$\alpha$	$\beta$	$\gamma$
Exact Values	1200.0	0.0100	1.0000	0.2000
Initial guesses	600.0	0.0050	0.5000	0.1000
w/ 2-modes	1156.8	0.0096	0.4956	0.1674
w/ 5-modes	1174.2	0.0096	0.4894	0.1789
w/ 12-modes	1167.8	0.0096	0.5509	0.1789

matrix  $P_{0/0}$  and the system and the observation noise covariance matrices  $Q$  and  $R$  were taken as diagonal matrices with 0.01 in their diagonals. Table 3 shows two estimated nonlinear parameters using various numbers of the sorted modes and SMEKF. The results indicate that the accuracy of the estimated parameters got improved with the increasing number of the modes included. Reasonable estimates of the parameters were obtained with the SMEKF, which can reproduce excellent hystereses

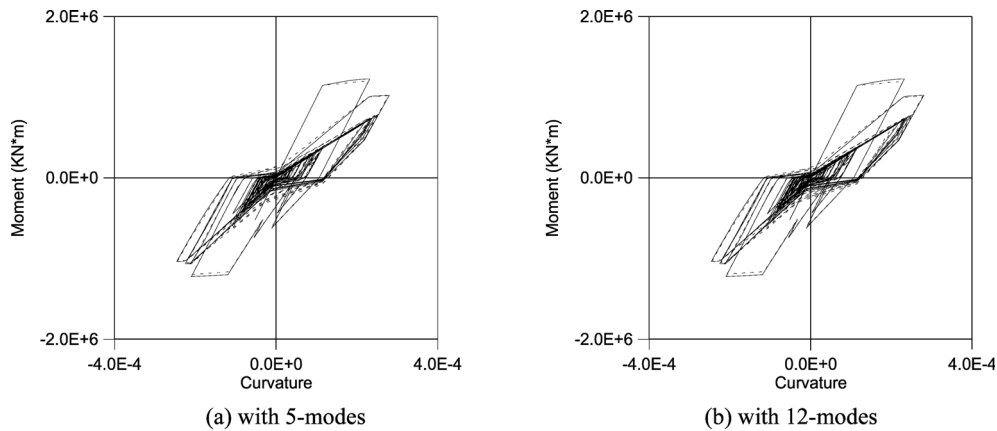


Fig. 17 Estimated  $M-\phi$  relationships by the SMEKF and modal sorting (—: Exact and ----: Recalculated)

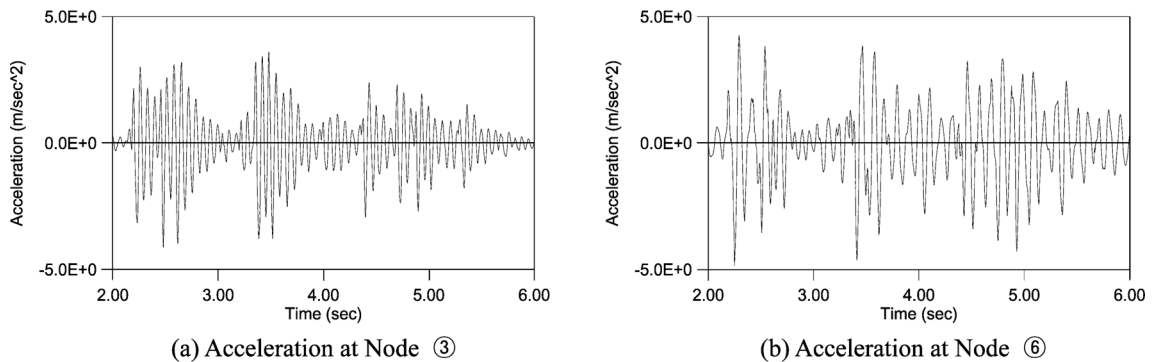


Fig. 18 Recalculated acceleration responses by the SMEKF with 12 sorted modes (2-6sec; —: Exact and ----: Recalculated)

as shown in Fig. 17. In Fig. 18, the recalculated acceleration responses with the identified parameters using 12 sorted modes are compared with the exact responses. It can be found that very accurate responses have been estimated.

Fig. 19 shows the tracking procedures of the parameter estimation in global iterations. In the present case, the nonlinear parameters have been estimated by increasing the number of the included sorted modes. So the estimated parameters were reused as the initial guesses for the next identification procedure which included more modes. Fig. 19 shows that the yield moment and post yield stiffness parameters ( $M_y$  and  $\alpha$ ) were reasonably identified with the two sorted modes. The strength deterioration parameter  $\gamma$  was found to converge to an exact value, if 5 sorted modes were used. Fig. 19(c) shows that the pinching parameter  $\beta$  was identified at the last stage of identification which included 12 sorted modes. The accuracy of the estimate for  $\beta$  is not so good as shown in Table 4. However, very good estimate has been obtained for the hysteresis as shown in Fig. 17, which indicates the insensitivity of the parameter for the overall hysteretic behavior in the present example case.

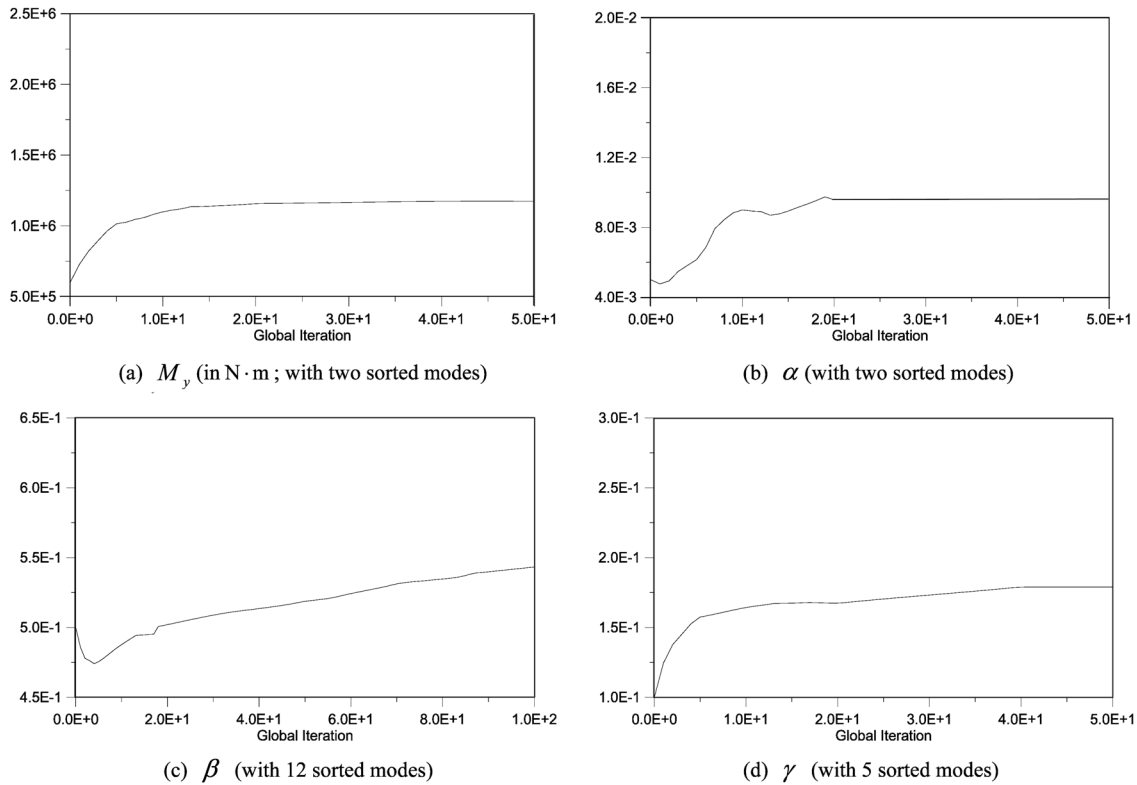


Fig. 19 Parameter tracking procedures in global iterations by the SMEKF with sorted modes

## 6. Conclusions

In this study, identification of the nonlinear hysteretic behavior of a RC bridge pier is carried out. The hysteretic behavior is modeled using the modified Takeda model, in which important nonlinear characteristics of the damaged RC pier, such as stiffness degradation, pinching effect and strength deterioration, can be effectively described using a limited number of parameters. As the modified Takeda model logically defined the hysteresis with various rules of loading and reloading, the modified extended Kalman filter (MEKF) is employed instead of the conventional extended Kalman filter (EKF), in which a finite difference scheme is used for calculating the state transition matrix. In this study, a mode superposition method with modal sorting is proposed to reduce the problem size for the nonlinear system identification using Kalman filtering techniques. The sequential modified extended Kalman filter (SMEKF) is also proposed to improve the convergence and to prevent the erroneous estimation results in practical structural dynamic system with a large number of DOFs, in which the MEKF is used for the state estimation and the nonlinear sequential prediction error method is for the parameter identification.

Example analyses were carried out on a continuous bridge with a RC pier in the middle, which is subjected to earthquake excitations in the longitudinal and transverse directions. It has been found that both of the SMEKF and a mode superposition with modal sorting technique are very effective to identify the nonlinear hysteretic behavior and parameters involved in a locally damaged bridge pier

with a limited measurement data for the acceleration responses of the bridge structure. The system identification for nonlinear structural dynamic systems was customarily carried out with displacement or velocity responses. However, in this study a nonlinear parameter identification method has been developed using the acceleration measurements only, which are much easier to measure in the practical bridge structures, such as long-span bridges.

## Acknowledgements

This study has been supported by the Smart Infra-Structure Technology Center established at KAIST under the sponsorship of the Korea Science and Engineering Foundation. The support is greatly acknowledged.

## References

- Aprile, A., Benedetti, A. and Trombetti, T. (1994), "On non-linear dynamic analysis in the frequency domain: algorithms and applications", *Earthq. Eng. Struct. Dyn.*, **23**, 363-388.
- Atalay, M.B. and Penzien, J. (1975), "The seismic behavior of critical regions of reinforced concrete components influenced by moment, shear and axial force", Earthquake Engrg. Research Center Report No. EERC 75-19, Univ. of California, Berkeley, Calif.
- Baber, T.T and Wen, Y.K. (1981), "Random vibration of hysteretic degrading systems", *J. Eng. Mech. Div., ASCE*, **107**(EM6), 1069-1087
- Blumin, S.L. and Pogodaev, A.K. (2003), "Recursive iterative algorithms for adaptive identification of nonlinear concentrated dynamic systems", *Automation and Remote Control*, **64**(10), 1583-1588.
- Clough, R.W., Benuska, K.L. and Wilson E.L. (1965), "Inelastic earthquake response of tall buildings", *Proc., 3rd world Conf. on Earthq. Eng.*, New Zealand, II, 68-89.
- Chung, Y.S., Meyer, C. and Shinozuka, M. (1989), "Modeling of concrete damage", *ACI Struct. J.*, **86**(3), 259-271.
- D'Ambrisi, A. and Filippou, F.C. (1999), "Modeling of cyclic shear behavior in RC members", *J. Struct. Eng., ASCE*, **125**(10), 1143-1150.
- D'Aveni, A. and Muscolino, G. (2001), "Improved dynamic correction method in seismic analysis of both classically and non-classically damped structures", *Earthq. Eng. Struct. Dyn.*, **30**, 501-517.
- Dikens, J.M., Nakagawa J.M., and Wittbrodt M.J. (1981), "A critique of mode acceleration and modal truncation argumentation methods for modal response analysis", *Comput. Struct.*, **62**(6), 985-998.
- Goodwin, G.C. and Sin, K.S. (1984), *Adaptive filtering prediction and control*, Information and System Science Series.
- Hoshiya, M., and Saito, E. (1984), "Structural identification by extended Kalman filter", *J. Eng. Mech., ASCE*, **110**(12), 1757-1770.
- Kwak, H.G., Kim, S.P. and Kim, J.E. (2004), "Nonlinear dynamic analysis of RC frames using cyclic moment curvature relation", *Struct. Eng. Mech.*, **17**(3-4), 357-378.
- Kunnath, S.K., Reinhorn, A.M. and Park, Y.J. (1990), "Analytical modeling of inelastic seismic response of R/C structures", *J. Struct. Eng., ASCE*, **116**(4), 996-1017.
- Lee, C.G. and Yun, C.B. (1991), "Parameter identification of linear structural dynamic systems", *Comput. Struct.*, **40**(6), 1475-1487.
- Loh, C.H. and Chung, S.T. (1993), "A three stage identification approach for hysteretic systems", *Earthq. Eng. Struct. Dyn.*, **22**, 129-150.
- Loh, C.H. and Lee, Z.K. (1997), "Seismic monitoring of a bridge : Assessing dynamic characteristics from both weak and strong ground excitations", *Earthq. Eng. Struct. Dyn.*, **26**, 269-288.

- Ma, S.M., Bertero, V.V. and Popov, E.P. (1976), "Experimental and analytical studies on the hysteretic behavior of reinforced concrete rectangular and T-beams", Earthquake Engrg. Research Center Report No. EERC 76-2, Univ. of California, Berkeley, Calif.
- Meyer, C., Roufaiel, M.C.L. and Arzoumanidis, S.G. (1983), "Analysis of damaged concrete frames for cyclic loads", *Earthq. Eng. Struct. Dyn.*, **11**, 207-228.
- Mohraz, B., Elghadamsi, F.E. and Chang, C.J. (1991), "An incremental mode-superposition for nonlinear dynamic analysis", *Earthq. Eng. Struct. Dyn.*, **20**, 471-481.
- Nørgaard, M., Poulsen, N.K. and Ravn, O. (2000), "New developments in state estimation for nonlinear systems", *Automatica*, **36**, 1627-1638.
- Mork, K.J. (1994), "Response analysis of reinforced concrete structures under seismic excitation", *Earthq. Eng. Struct. Dyn.*, **23**, 33-48.
- Otani, S. and Sozen, M.A. (1972), "Behavior of multistory reinforced concrete frames during earthquake", Tech. Report Strut. Res. Series No. 392, Univ. of Illinois, Urbana, Ill.
- Ozcebe, G. and Saatcioglu, M. (1989), "Hysteretic shear model for reinforced concrete members", *J. Struct. Eng.*, ASCE, **115**(1), 132-148.
- Park, R., Kent, D.C. and Sampton, R.A. (1972), "Reinforced concrete members with cyclic loading", *J. Struct. Div.*, ASCE, **98**(7) 1341-1360.
- Popov, E.P., Bertero, V.V. and Krawinkler, H. (1972), "Cyclic behavior of three R.C flexural members with high shear", Earthquake Engrg. Research Center Report No. EERC 72-5, Univ. of California, Berkeley, Calif.
- Roufaiel, M.S.L. and Meyer, C. (1987), "Analytical modeling of hysteretic behavior of R.C. frames", *J. Struct. Eng.*, ASCE, **113**(3), 429-443.
- Sato, T. and Qi, K. (1998), "Adaptive  $H_\infty$  filter: Its application to Structural Identification", *J. Eng. Mech.*, ASCE, **124**(11), 1233-1240.
- Sato, T. and Takei, K. (1998), "Development of a Kalman filter with fading memory", *Struct. Safety and Reliability*, 387-394.
- Sato, T. and Chung, M. (2005), "Structural identification using adaptive Monte Carlo filter", *J. Struct. Eng.*, JSCE, **51**(A), 471-477.
- Schei, T.S. (1997), "A finite-difference method for linearization in nonlinear estimation algorithm", *Automatica*, **33**(11), 2053-2058.
- Smyth, A.W., Masri, S.F., Chassiakos, A.G. and Caughey, T.K. (1999), "On-line identification of MDOF nonlinear hysteretic systems", *J. Eng. Mech.*, ASCE, **125**(2), 133-142.
- Takeda, T., Sozen, M.A. and Nielsen, N. N. (1970), "Reinforced concrete response to simulated earthquakes". *J. Struct. Div.*, ASCE, **96**(12), 2557-2573.
- Umemura, H. and Takizawa, H. (1982), "Dynamic response of reinforced concrete buildings", *International Association of Bridge and Struct. Engrg.*, Zürich, Switzerland.
- Villaverde, R. and Hanna, M. M. (1992), "Efficient mode superposition algorithm for seismic analysis of non-linear structures", *Earthq. Eng. Struct. Dyn.*, **21**, 849-858.
- Wight, J.K. and Sozen, M.A. (1975), "Strength decay of RC columns under shear reversal", *J. Struct. Div.*, ASCE, **101**(5), 1053-1065.
- Wilson, E.L. (2002), *Static and Dynamic Analysis of Structures*, Computer and Structures Inc.
- Wilson, E.L., Yuan, M.W. and Dickens, J.M. (1982), "Dynamic analysis by direct superposition of Ritz vectors", *Earthq. Eng. Struct. Dyn.*, **10**, 813-821.
- Yang, J.N., and Lin, S. (2005), "Identification of parametric variations of structures based on least squares estimation and adaptive tracking technique", *J. Eng. Mech.*, ASCE, **131**(3), 290-298.
- Yang, J.N., Lin, S., Huang, H. and Zhou, L., (2006), "An adaptive extended Kalman filter for structural damage identification", *Struct. Control Health Monit.*, **13**(4), 849-867.
- Yang, J.N., Huang, H., and Lin, S. (2006), "Sequential nonlinear least-square estimation for damage identification of structures", *Int. J. Nonlinear Mech.*, **41**, 124-140.
- Yang, J.N. and Huang, H. (2007), "Sequential non-linear least-square estimation for damage identification of structures with unknown inputs and unknown outputs", *Int. J. Non-linear Mech.*, **42**, 789-801.
- Yar, M. and Hammond, J.K. (1986), "Modeling and response of bilinear hysteretic systems", *J. Eng. Mech.*, ASCE, **113**(7), 1000-1013.

- Yoshida, I. and Sato, T. (2002), "Health monitoring algorithm by the Monte Carlo filter based on non-Gaussian noise", *J. Nat. Disaster Science*, **24**(2), 101-107.
- Yun, C. B. and Lee, H.J. (1997), "Substructural identification for damage estimation of structures", *Struct. Safety*, **19**(1), 121-140.
- Yun, C.B., Lee, H.J. and Lee, C.G. (1997), "Sequential prediction error method for structural identification", *J. Eng. Mech.*, ASCE, **123**(2), 115-123.
- Yun, C.B. and Shinozuka, M. (1980), "Identification of nonlinear structural dynamic systems", *J. Struct. Mech.*, ASCE, **8**(ST2), 187-203.

CC